



CrossMark
 click for updates

Cite this: *RSC Adv.*, 2015, 5, 51116

Improved thermal properties of borosilicate glass composite containing single walled carbon nanotube bundles

Sujan Ghosh, Arnab Ghosh, Jonaki Mukherjee and Rajat Banerjee*

A single walled carbon nanotube (SWCNT) incorporated borosilicate glass composite was fabricated by a melt quench technique. The thermal diffusivity, specific heat and the thermal conductivity of the base glass and the composite were determined together with their temperature profile. Enhancement of the diffusivity and the conductivity in the composite was found compared to that of the base glass. The interfacial thermal resistance (R_k) plays a decisive role in the thermal transport properties of the composite. Furthermore, the effect of phonons was discussed to substantiate the transport mechanism and the temperature profile of different thermal parameters.

Received 18th March 2015

Accepted 2nd June 2015

DOI: 10.1039/c5ra04810a

www.rsc.org/advances

1 Introduction

The problem of thermal transport in composite materials is driving renewed interest among several researchers in this decade. Applications include high performance thermal transfer materials and heat dissipation in microelectronics demands not only efficient thermal management, but also a better fundamental understanding of the underlying physical mechanisms. In recent years, many researchers have fabricated advanced composite materials filled with SWCNTs keeping in mind the remarkable thermal properties of the nanotubes such that the materials can have enhanced thermal parameters than that of the base matrix. In most of the cases polymers or metals were chosen as the host materials into which the nanotubes were incorporated.^{1,2} Several reports were also available regarding the thermal-transfer liquids containing carbon nanotubes in suspended form.^{3,4} However, very few works were reported on the thermal properties of the CNT-ceramics or the CNT-glass composites.^{5,6} Some of the attempts were failed to improve the thermal properties of CNT-composites.^{7,8} Even the increment was not sufficient in all the successful efforts with respect to the intrinsic thermal conductivity of the individual SWCNTs. Previous reports suggest that the thermal boundary resistance between the filler and the matrix is the prime responsible factor for these circumstances. In this report, we describe the thermal properties of the borosilicate glass and the SWCNT-borosilicate glass composite including thermal diffusivity, specific heat and the thermal conductivity. The behaviors of all these thermal parameters were studied at room temperature and higher temperature environment. The prime interest

of this study was to analyze the functions of SWCNTs in the composite so that it can be considered as a prospective material for thermal interface⁹ and heat sinking applications.¹⁰ The effects of high temperature on the different thermal parameters were another significant intention of this work. In this context, the thermal boundary resistance and the interaction of phonons were thoroughly discussed to realize the fundamental physics behind the thermal transport in the composite material.

2 Experimental

90% pure SWCNTs were commercially purchased from Arry, Germany having length $\sim 5\text{--}20\ \mu\text{m}$, OD-1-2 nm and thermal conductivity $\sim 4000\ \text{W mK}^{-1}$. 0.1 g of SWCNT is taken in a mixture of aniline and toluene. The mixture was heated and refluxed to disperse the SWCNTs in the solvent and the solution became dark brown. Borosilicate glass of following composition ($\text{SiO}_2\text{-}69.2\%$, $\text{B}_2\text{O}_3\text{-}10\%$, $\text{K}_2\text{O}\text{-}8.4\%$, $\text{BaO}\text{-}3\%$, $\text{Na}_2\text{O}\text{-}8.9\%$, $\text{CeO}_2\text{-}0.53\%$) was selected as the host matrix for the fabrication of the glass composites. The glass transition temperature and softening point of the glass was found to $567\ ^\circ\text{C}$ and $717\ ^\circ\text{C}$ respectively. Pieces of glass (3 to 5 mm dimension) was taken in a carbon crucible and properly mixed with the definite volume of the prepared SWCNT solution. The wetted glass is melted by melt quench technique in an atmospheric controlled furnace at $790\text{--}810\ ^\circ\text{C}$ for 1 hour and then rapidly cooled to room temperature to avoid the crystal phases in the composite. The same root was adopted for the synthesis of SWCNT-glass composite as described in our previous report.¹¹ After the fabrication the thermal diffusivity and the specific heat of the base glass and the composite were determined through the Laser flash method (Model no. Flash line-4010, Anter corporation: USA) where gold coated samples were used. The thermal

Central Glass and Ceramic Research Institute, Jadavpur, Kolkata-700 032, India.
 E-mail: rajatbanerjee@hotmail.com; Fax: +9133 24730957; Tel: +9133 24838079 ext. 3255

data was measured in an inert atmosphere of Argon gas in the temperature range 300 to 683 K. Archimedes principle was used to determine the density (ρ) of the base glass and the composite. For this purpose the mass (M) of the specimens (in air) was determined by a balance. Then, partially water filled volumetric cylinder was taken and the reading of the water level was observed before and after immersion of the material. From the difference of these readings the volume (V) of the materials was measured. So, after determining the mass and the volume of the specimens, the density was calculated by the formula $\rho = M/V$. The volume fraction of the SWCNTs has been evaluated by calculating the total volume of the composite and the volume of SWCNT used and was found to be 0.7% for the fabricated composite.

3 Results and discussions

3.1 Thermal diffusivity

Thermal diffusivities (D) of the composite along with the base glass were plotted with different temperatures in Fig. 1, where it can be observed that the diffusivities were almost temperature independent in this range. Further, one can easily examine that the composite show higher diffusivity than that of their base glass. Other researchers also reported the similar trend in different CNT composites.¹² Actually, a small part of the incident heat was absorbed by the nanotubes and the rest was transferred into the present medium around the tubes.

3.2 Specific heat capacity

Fig. 2 shows the temperature dependent specific heat capacity (C_p) of the base glass and composite, where small reduction was observed in C_p for the composite than that of the base glass. Similar results were obtained in MWCNT/nylon-6 composites¹³ and SWCNT/polyisoprene composite.¹⁴ The above phenomena clearly indicate that carbon nanotubes suppress the heat capacity of the host matrix due to the weak van der Waals

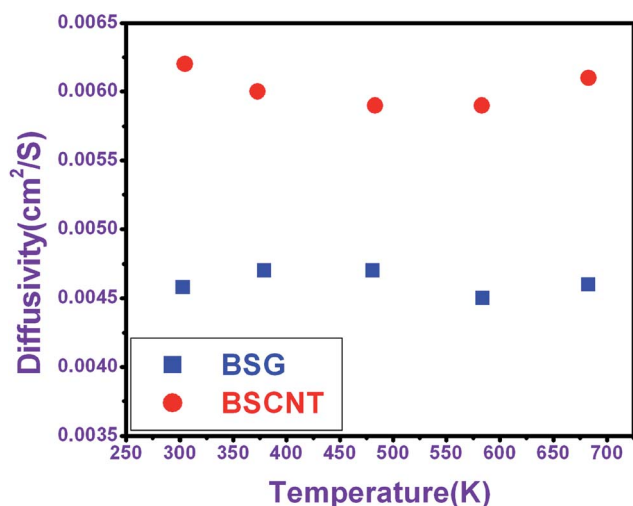


Fig. 1 Diffusivity vs. temperature plot for borosilicate glass (BSG) and SWCNT-borosilicate glass composite (BSCNT).

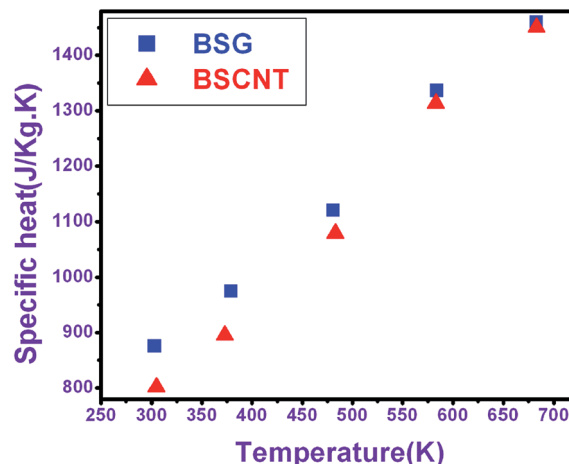


Fig. 2 Specific heat vs. temperature plot for borosilicate glass (BSG) and SWCNT-borosilicate glass composite (BSCNT).

interaction between the nanotubes and the base materials. Moreover, acute observation at the high temperature region reveals that the difference in C_p for the base glass and their composite was significantly reduced in this range. Actually specific heat of CNTs raises sharper with the increase in temperature than that of the base glass.¹⁵

3.3 Thermal conductivity

Thermal conductivity (K) was calculated by the following equation after determining the thermal diffusivity (D) and the specific heat capacity (C_p)

$$K = D\rho C_p \quad (1)$$

of the materials by the laser flash method. On the other hand ρ denotes the density of the specimens determined through the Archimedes principle and was found to be 2.23 and 2.16 g cm⁻³ for the base glass and the composite respectively. Temperature profile of the thermal conductivities for the base glass and the composite were shown in Fig. 3 where linear rise of the thermal conductivity was observed for both the specimens. Similar increment of the thermal conductivity was found in other reports dealing with CNT-polymer¹⁶ and in CNT based nano-fluid.¹⁷ Furthermore, it illuminates from Fig. 3 that the liner fits of the thermal conductivity were not parallel and the slopes were found to be 0.00107 and 0.00272 for the base glass and the composite respectively. It implies that at room temperature the difference in the thermal conductivity between borosilicate glass and the composite was small, but as temperature rises the difference became more pronounced. However, about 33% increment of the thermal conductivity was observed in the composite than that of the base glass at 683 K.

3.4 Effect of thermal boundary resistance in thermal conductivity

Meticulous research on the thermal transport in CNT composites reveals the fact that thermal boundary resistance (known as Kapitza resistance) plays a significant role to determine the

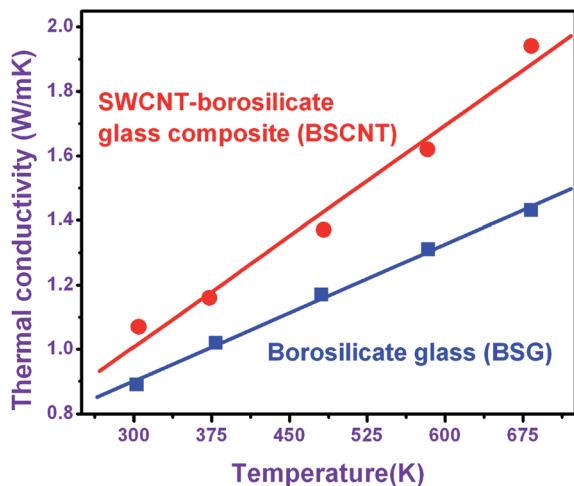


Fig. 3 Thermal conductivity vs. temperature plot for borosilicate glass and SWCNT–borosilicate glass composite.

effective thermal conductivity of the composites. In this concern one can think about CNT–CNT and CNT–matrix interfacial resistance. However, CNT–CNT interfacial resistance is dominant in those composites where nanotube bundles were aligned in a certain direction.¹⁸ Conversely, for the random distribution of nanotube bundles CNT–matrix interfacial resistance is dominated in transport process. So, considering the Kapitza resistance (R_k) at the interface between nanotubes and the base material, different models^{19–22} have been proposed to explain the fundamental physical mechanisms for the thermal transport in composite materials. Among those approaches, Effective Medium Theory was particularly useful for the composites containing random distribution of CNTs. In this context the surface morphology of SWCNT–borosilicate glass composite is shown in the FESEM image (Fig. 4). Simple inspection of the figure clearly illuminates that the nanotubes were embedded in the glassy envelope in the form of bundles and distributed throughout the composite with completely random manner.

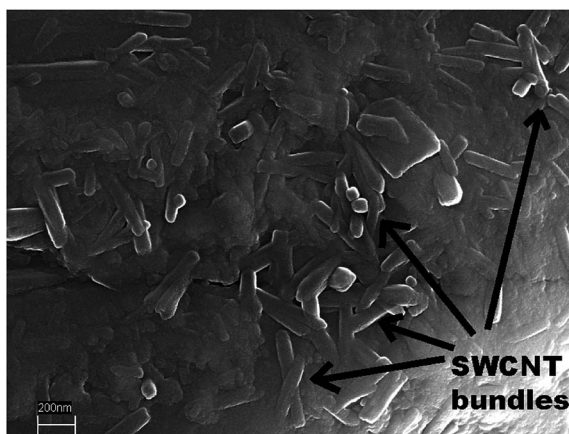


Fig. 4 FESEM image of SWCNT–borosilicate glass composite showing random distribution of SWCNT bundles throughout the composite.

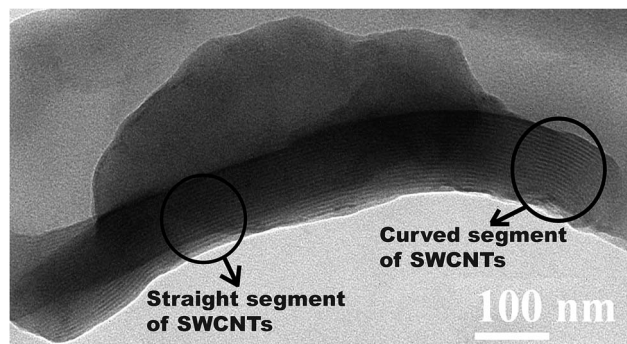


Fig. 5 HRTEM image of SWCNT–borosilicate glass composite showing the straight and curved portion of individual nanotubes inside a bundle.

One can also observed the entanglement of the SWCNT bundles all through the glass host which further build the basis of the tube–tube thermal resistance in the thermal transport through the composite. In this scenario the actual condition of the individual nanotubes was very much significant for details scrutiny of this phenomenon. For this reason the SWCNT bundles were further analyzed by the HRTEM image (Fig. 5) where one can see the straight and the non-straight segments of an individual nanotube.

Considering the random distribution and the non-straightness of CNTs, Deng *et al.*²³ recommended a model based on the effective medium approach. By this model one can determine the effective thermal conductivity (K_e) of a composite material taking into consideration the thermal conductivity of the base material (K_m), volume fraction of CNT in the composite (f), the straightness ratio (η) and the aspect ratio (p) of the nanotubes. The model introduces a special function H for the influence of η and p as shown in eqn (2). Here, K_{33}^{cs} represents the modified form of transverse thermal conductivity (K_{33}^c) and arises from the tube end thermal resistance.²⁴ Eqn (3) indicates the relation between K_{33}^{cs} and K_{33}^c . Moreover, the straightness ratio can be evaluated by eqn (4) where L and L^{ce} denote the original and the effective length of CNTs. The effective thermal conductivity

$$\frac{K_e}{K_m} = 1 + \frac{\eta f}{\frac{K_m}{\eta K_{33}^{cs}} + H(\eta p)} \quad (2)$$

$$\text{where } K_{33}^{cs} = \frac{K_{33}^c}{\left(1 + \frac{2R_k K_{33}^c}{L}\right)} \quad (3)$$

$$\text{and } \eta = \frac{L^{ce}}{L} \quad (4)$$

of SWCNT–borosilicate glass composite was evaluated by eqn (2) allowing for $\eta = 0.3$ and $R_k = 8 \times 10^{-8} \text{ m}^2\text{K W}^{-1}$, where in this composite $f = 0.7\%$, $K_{33}^c = 4000 \text{ W mK}^{-1}$, $K_m = 1.43 \text{ W mK}^{-1}$ at 683 K and the average aspect ratio of CNT is 6250. Taking into account the above mentioned values of the different parameters the model predicts that the ratio of K_e and K_m

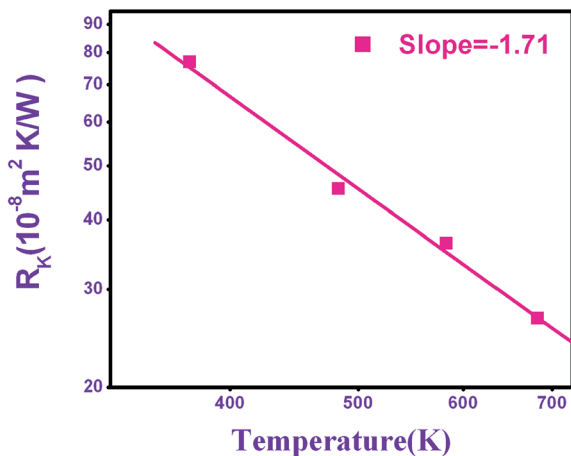


Fig. 6 Log-log plot of R_k vs. temperature for the fabricated composite to determine the non linearity.

should be 1.44 at 683 K. On the other hand, at this temperature the experimental value of K_e/K_m was found to be 1.37. So, this model almost diminishes the anomaly between the experimental results and the theoretical calculation. Similar prediction by this model was found to be almost accurate in different experiments including our previous work.^{4,25} However, in this framework, it will be also interesting to investigate the character of R_k with increasing temperature. One can easily estimate the approximate values of R_k (for this composite) at different temperatures by putting the experimental values of K_e and K_m in eqn (2) and (3), whether keeping all other parameters same. Fig. 6 illustrates the R_k versus temperature plot in log-log scale where nonlinear decrease of R_k was found with increasing temperature. Similar nature of reduction was found in different composites with solid-solid²⁶ and solid-liquid²⁷ interfaces.

3.5 Role of phonons in thermal conduction

Phonons are dominating in thermal transport process both for glass^{28,29} and carbon nanotubes.³⁰ Moreover, above room temperature the mechanism is fully controlled by the localized phonons in glass.²⁹ However, a frequency mismatch takes place between the phonons of dissimilar materials in case of the composite which can be one of the reasons for the boundary resistance in thermal conduction. This type of difficulty in different composites was comprehensively reviewed by Swartz and Pohl in their report.³¹ In this context, the acoustic mismatch model (AMM) and the diffuse mismatch model (DMM) were frequently used specially for the composites where two or more dissimilar materials intermixed with each other. The effects of intermixing on the thermal conduction were investigated in different reports³²⁻³⁵ where aforesaid models were thoroughly utilized to understand the thermal transport at the molecular level. In short, AMM assumes that the phonons were governed by continuum acoustics and the interface was considered as a plane surface. In this approach the interfacial region was treated as a perfectly smooth wall where only specular interactions and transmission were believed to occur

between the phonon waves. Thus, the possibility of scattering at the interface was ignored in this theory. However, investigations on various composites revealed that AMM was only valid for the mixture of similar solids where the interfaces were considered almost continuum medium such that the idea of specular reflections can take place in those regions. Also, different experiments suggest that above 30 K temperature the prediction by this model were far from the reality.³⁶ Hence, AMM cannot be applicable in the case of SWCNT-borosilicate glass composite due to the imperfections and roughness presents at the interfacial regions. In addition, the experiments were carried out at such temperature range (>30 K) where AMM was not valid. So a question can invariably arises that how one can explain the significant increment of the thermal conductivity in this composite? Now, considering another model namely DMM, which deals with the completely opposite idea compared to AMM. In DMM, the absolute specular nature of the interfaces was never considered as because of the imperfections presents in that area. Consequently scattering became an obvious phenomenon in this situation which totally destroys the correlation between the wave vectors of incoming and the outgoing phonons. Moreover this model predicts that the scattering enhanced the thermal boundary resistance in composites containing very similar solids whereas a significant reduction of the boundary resistance occurs by this scattering in a mixture of dissimilar materials. Therefore, the diffused scattering plays completely the opposite role in two type of intermixing as discussed in several reports.^{31,34,37} Further, the experiments on the thermal transport for the mixture of dissimilar solids suggest that DMM was much closer to the experimental data for a wide temperature range though it assumes only the elastic scattering between the phonons. So, the above analysis clearly illuminates that DMM is the most reasonable approach for the thermal transport in SWCNT-borosilicate glass composite. Here the nanotubes exhibits higher frequency phonons compared to the base material which further initiate the interface effect in this composite. Evidences like bundle formation and the entanglement of carbon nanotubes (as shown in Fig. 4) ensures the diffusive nature of the phonons at the interface. Further one can think about the inelastic phonon scattering at the interfacial region as suggested by different workers.³⁸⁻⁴⁰ It implies that the phonons in nanotubes at frequencies higher than the maximum phonon frequency of the base glass do also participate in the transport mechanism. Now considering the inelastic scattering within the diffused environment of phonons it can be stated that at room temperature the scattering of phonons is lower and the composite experienced maximum interface effect. For this reason thermal conductivity enhancement in the composite was lower at this regime (Fig. 3). Moreover, as temperature rises the thermal agitations became higher which effectively increased the phonon scattering at the intermixing regions of CNT and glass in the composite. This enhanced scattering at higher temperature consequently reduced the interface resistance around the different boundaries within the material. Thus, the thermal profile of R_k (Fig. 6) clearly corroborates this fact. Also, the reduced difference in C_p for the base glass and the

composite at higher temperature substantiate the enhanced phonon scattering at this range.

4 Conclusion

Scrupulous investigation was performed to understand the basic mechanism behind the absorption and the transport of thermal energy in SWCNT incorporated borosilicate glass composite. The thermal transport through the nanotubes was found to be experienced considerable obstacle by the thermal boundary resistance (TBR) at the interface between the nanotubes and the glassy matrix. In spite of that, the thermal diffusivity and the thermal conductivity were appreciably enhanced in the composites, where the enhancement was more pronounced at higher temperature regime. However, the entire phenomena were clearly enlightened under the phonon transport mechanism through the diffuse mismatch model and considering the inelastic scattering of phonons at the interface. Frequency mismatch between the phonons of different material was proposed to be the fundamental basis of the thermal boundary resistance. Further, the enhanced thermal transport at the higher temperature was explicated by the temperature dependent scattering of phonons at the interface. These interesting experimental findings elucidate that the SWCNT incorporated borosilicate glass composite can be considered as the potential materials for the thermal interface and the heat sinking applications in microelectronics. Though, the real fabrication of the devices is the topic of further research.

Acknowledgements

The authors are grateful to Prof. Dr Indranil Manna, former Director of Central Glass & Ceramic Research institute (CGCRI) for his constant encouragement to execute this work. Heartfelt thanks are given to Mr Kamal Dasgupta, Acting Director, C.G.C.R.I. for his continuous support to carry out the work. They also acknowledge Mr Amit Sarkar, Mr Sudipta Mandal, Mr Ranadhir Bose and Mr Amal Datta from CRF of IIT Kharagpur for attractive HRTEM micrographs, Mr Sumantra Basu of NOCCD, CGCRI for instrumental set up in thermal diffusivity measurement and Mr Ashoke Mandal in ESM division of CGCRI for FESEM micrograph.

References

- Z. Li, W. Wu, H. Chen, Z. Zhu, Y. Wang and Y. Zhang, *RSC Adv.*, 2013, **3**, 6417.
- X. L. Shi, H. Yang, G. Q. Shao, X. L. Duan, L. Yan, Z. Xiong and P. Sun, *Mater. Sci. Eng., A*, 2006, **457**, 18.
- B. Gu, B. Hou, Z. Lu, Z. Wang and S. Chen, *Int. J. Heat Mass Transfer*, 2013, **64**, 108.
- S. U. S. Choi, Z. G. Zhang, W. Yu, F. E. Lockwood and A. Grulke, *Appl. Phys. Lett.*, 2001, **79**, 2252.
- L. Kumari, T. Zhang, G. H. Du, W. Z. Li, Q. W. Wang, A. Datye and K. H. Wu, *Compos. Sci. Technol.*, 2008, **68**, 2178.
- A. Mukhopadhyay, G. Otieno, B. T. T. Chu, A. Wallwork, M. L. H. Green and R. I. Todd, *Scr. Mater.*, 2011, **65**, 408.
- G. D. Zhan and A. K. Mukherjee, *Int. J. Appl. Ceram. Technol.*, 2004, **1**, 161.
- S. R. Bakshi, K. Blani and A. Agarwal, *J. Am. Ceram. Soc.*, 2008, **91**, 942.
- J. Xu and T. S. Fisher, *Int. J. Heat Mass Transfer*, 2006, **49**, 1658.
- J. Hone, M. C. Llaguno, M. J. Biercuk, A. T. Johnson, B. Batlogg, Z. Banes and J. E. Fischer, *Appl. Phys. A*, 2002, **74**, 339.
- A. Ghosh, S. Ghosh, S. Das, P. K. Das, D. D. Majumder and R. Banerjee, *Chem. Phys. Lett.*, 2010, **496**, 321.
- K. Kappagantula and M. L. Pantoya, *Int. J. Heat Mass Transfer*, 2012, **55**, 817.
- J. Yu, B. Tonpheng, G. Grobner and O. Anderson, *Carbon*, 2011, **49**, 4858.
- B. Tonpheng, J. Yu and O. Anderson, *Macromolecules*, 2009, **42**, 9295.
- J. Hone, in *Phonons and thermal Properties of Carbon Nanotubes, Carbon Nanotubes*, ed. M. S. Dresselhaus and G. Dresselhaus, *Appl. Phys.*, Springer-Verlag Berlin, 2001, vol. 80, p. 273.
- M. B. Jakubinek, M. A. White, M. Mu and K. I. Winey, *Appl. Phys. Lett.*, 2010, **96**, 083105.
- F. C. Li, J. C. Yang, W. W. Zhou, Y. R. He, Y. M. Huang and B. C. Jiang, *Thermochim. Acta*, 2013, **556**, 47.
- H. Zhong and J. R. Lukes, *Phys. Rev. B: Condens. Matter Mater. Phys.*, 2006, **74**, 125403.
- Y. S. Song and J. R. Youn, *Carbon*, 2006, **44**, 710.
- C. W. Nan, *Prog. Mater. Sci.*, 1993, **37**, 1.
- C. W. Nan, R. Birringer, D. R. Clarke and H. Gleiter, *J. Appl. Phys.*, 1997, **81**, 6692.
- N. Nishimura and Y. J. Liu, *Comput. Mech.*, 2004, **35**, 1.
- F. Deng, Q. S. Zheng, L. F. Wang and C. W. Nan, *Appl. Phys. Lett.*, 2007, **90**, 021914.
- T. Chen, G. J. Weng and W. C. Liu, *J. Appl. Phys.*, 2005, **97**, 104312.
- S. Ghosh, A. Ghosh, T. Kar, S. Das, P. K. Das and R. Banerjee, *Chem. Phys. Lett.*, 2012, **547**, 58.
- M. A. Panzer, H. M. Duong, J. Okawa, J. Shiomi, B. L. Wardle, S. Maruyama and K. E. Goodson, *Nano Lett.*, 2010, **10**, 2395.
- G. Song and C. Min, *Mol. Phys.*, 2013, **111**, 903.
- G. S. Dixon, B. D. Gault, S. Y. Shi, P. A. Watson and J. P. Wicksted, *Phys. Rev. B: Condens. Matter Mater. Phys.*, 1994, **49**, 257.
- W. P. Allen, J. D. Bromwell, T. Doyle, L. Devlin, R. Snider, P. Watson and G. Dixon, *Phys. Rev. B: Condens. Matter Mater. Phys.*, 1994, **49**, 265.
- J. Hone, M. Whitney, C. Piskoti and A. Zettl, *Phys. Rev. B: Condens. Matter Mater. Phys.*, 1999, **59**, R2514.
- E. T. Swartz and R. O. Pohl, *Rev. Mod. Phys.*, 1989, **61**, 605.
- P. E. Hopkins, *ISRN Mech. Eng.*, 2013, **2013**, 682586.
- P. E. Hopkins, P. M. Norris, R. J. Stevens, T. E. Beechem and S. Graham, *J. Heat Transfer*, 2008, **130**, 062401.
- P. E. Hopkins, T. E. Beechem, J. C. Duda, K. Hattar, J. F. Lnefeld, M. A. Rodriguez and E. S. Piekos, *Phys. Rev. B: Condens. Matter Mater. Phys.*, 2011, **84**, 125408.

- 35 J. C. Duda, J. L. Smoyer, P. M. Norris and P. E. Hopkins, *Appl. Phys. Lett.*, 2009, **95**, 031912.
- 36 R. M. Costescu, M. A. Wall and D. G. Cahill, *Phys. Rev. B: Condens. Matter Mater. Phys.*, 2003, **67**, 054302.
- 37 E. T. Swartz and R. O. Pohl, *Appl. Phys. Lett.*, 1987, **51**, 2200.
- 38 P. E. Hopkins, *J. Appl. Phys.*, 2009, **106**, 013528.
- 39 Z. L. Wang, H. T. Mu, J. G. Liang and D. W. Tang, *Int. J. Therm. Sci.*, 2013, **74**, 53.
- 40 J. C. Duda, P. E. Hopkins, T. E. Beechem, J. L. Smoyer and P. M. Norris, *Superlattices Microstruct.*, 2010, **47**, 550.